



OPEN ACCESS

EDITED BY

Anders Hansen,
Technical University of Denmark, Denmark

REVIEWED BY

Adrian Florin Gal,
University of Agricultural Sciences and
Veterinary Medicine of Cluj-Napoca, Romania
Nuria Maria Novoa,
University of Salamanca Health Care
Complex, Spain

*CORRESPONDENCE

Kazushi Asano
✉ asano.kazushi@nihon-u.ac.jp

SPECIALTY SECTION

This article was submitted to
Veterinary Surgery and Anesthesiology,
a section of the journal
Frontiers in Veterinary Science

RECEIVED 13 August 2022

ACCEPTED 19 January 2023

PUBLISHED 07 February 2023

CITATION

Sakurai N, Ishigaki K, Terai K, Heishima T,
Okada K, Yoshida O, Kagawa Y and Asano K
(2023) Impact of near-infrared fluorescence
imaging with indocyanine green on the surgical
treatment of pulmonary masses in dogs.
Front. Vet. Sci. 10:1018263.
doi: 10.3389/fvets.2023.1018263

COPYRIGHT

© 2023 Sakurai, Ishigaki, Terai, Heishima,
Okada, Yoshida, Kagawa and Asano. This is an
open-access article distributed under the terms
of the [Creative Commons Attribution License
\(CC BY\)](https://creativecommons.org/licenses/by/4.0/). The use, distribution or reproduction
in other forums is permitted, provided the
original author(s) and the copyright owner(s)
are credited and that the original publication in
this journal is cited, in accordance with
accepted academic practice. No use,
distribution or reproduction is permitted which
does not comply with these terms.

Impact of near-infrared fluorescence imaging with indocyanine green on the surgical treatment of pulmonary masses in dogs

Naoki Sakurai¹, Kumiko Ishigaki¹, Kazuyuki Terai¹, Tatsuya Heishima¹, Kazuki Okada², Orié Yoshida¹, Yumiko Kagawa² and Kazushi Asano^{1*}

¹Laboratory of Veterinary Surgery, Department of Veterinary Medicine, College of Bioresource Sciences, Nihon University, Fujisawa, Japan, ²North Lab, Sapporo, Japan

Objectives: To investigate the intraoperative identification and complete resection of pulmonary masses, and to evaluate lymph node metastasis of pulmonary malignant tumors in dogs using indocyanine green (ICG) fluorescence imaging.

Methods: Forty dogs with pulmonary masses were included, all of which underwent surgical treatment. ICG fluorescence imaging was performed on pulmonary masses before lobectomy and the resection margins after lobectomy. In addition, ICG fluorescence of the excised masses and lymph nodes was evaluated in the shaded box. The fluorescence findings were compared with the histopathological diagnosis.

Results: Of 44 nodules resected from 40 dogs, 32 nodules were histopathologically diagnosed as lung adenocarcinoma, five were histiocytic sarcoma, three were undifferentiated sarcoma, two were malignant epithelial tumor metastases, one was carcinosarcoma, and one was a non-neoplastic lesion. Fluorescence was observed in all nodules. In addition to the main lesion, other fluorescent nodules were found in four dogs. Regarding the diagnostic accuracy of complete resection based on ICG fluorescence, the sensitivity was 67.7% and the specificity was 60.0%. The sensitivity and specificity of ICG fluorescence for the diagnosis of lymph node metastasis were 100 and 75.0%, respectively.

Conclusions: ICG fluorescence imaging might be a useful intraoperative diagnostic method to identify the location of tumors and lymph node metastasis, but not to evaluate complete tumor resection, in dogs with pulmonary malignant tumors.

KEYWORDS

dog, fluorescence, indocyanine green, pulmonary masses, lymph node

1. Introduction

Indocyanine green (ICG) is a cyanine fluorescent dye that emits light that peaks at approximately 835 nm when illuminated with near-infrared light (750–810 nm) (1). Intravenously administered ICG is selectively taken up by hepatocytes and excreted in bile without being subjected to metabolism, enterohepatic circulation, or renal excretion. In human medicine, it has been recently shown that near-infrared fluorescence imaging using ICG has various applications, such as intraoperative identification and complete resection evaluation of hepatocellular carcinoma (2–4); identification of sentinel lymph nodes in various cancers such as breast, gastric, lung, and esophageal cancers (5–8); and patency of the graft for coronary artery disease (9). In veterinary medicine, the ICG fluorescence method has been used for identification

of 12 nodules of hepatocellular carcinoma in six dogs (10), identification of the thoracic duct in 15 dogs with chylothorax (11), examination of the intraoral sentinel lymph node in six hound dogs (12), intraoperative identification of epithelial bodies in three mongrel dogs (13), vascular visualization in caudal auricular flaps in two cats (14), and angiography for examining the normal ocular fundus in eight dogs (15). Nevertheless, several aspects of ICG imaging remain unclear owing to the relatively small number of reported studies and their small sample sizes.

Primary pulmonary tumors account for 1% of all tumors in dogs (16). Most primary pulmonary tumors are malignant and are most often bronchial or alveolar tumors; others include squamous cell carcinoma, histiocytic sarcoma, and anaplastic tumors (16–18). Surgical treatment is generally preferred for primary or metastatic tumors that are isolated (19). The median survival time (MST) for primary pulmonary tumors in dogs after surgical treatment is reported to be 361 days (18). It has also been reported that the MST of dogs with metastasis to the tracheobronchial lymph nodes is 26 days, while the MST of dogs without lymph node metastasis is significantly longer at 452 days (18). In another study, lymph node metastasis was identified as a prognostic factor (20). These data demonstrate the importance of determining the degree of infiltration and diagnosing lymph node metastasis when considering the prognosis of pulmonary tumors. The purposes of this study were to investigate the intraoperative identification and complete resection of pulmonary masses, and to evaluate lymph node metastasis of pulmonary malignant tumors in dogs using ICG fluorescence imaging.

2. Materials and methods

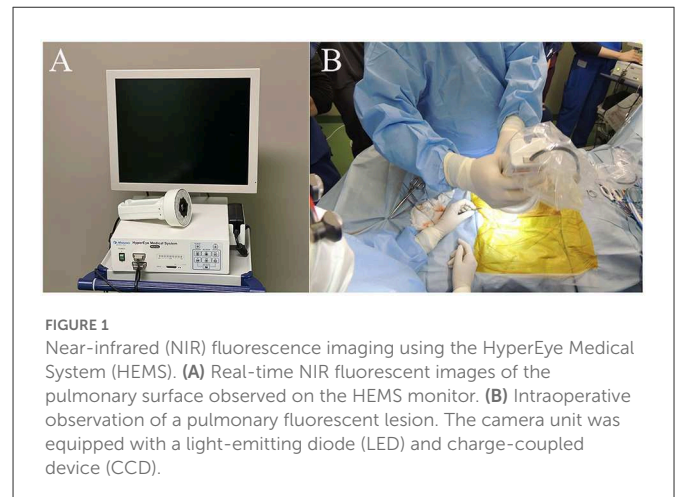
2.1. Animals and preoperative examination

This clinical case series study included 40 privately-owned dogs with pulmonary masses at the Animal Medical Center of Nihon University from November 2014 to January 2022. Informed consent was obtained from all owners, and information about all procedures was provided to the owners. All dogs underwent physical examination, blood count, serum chemistry tests, chest radiography, computed tomography (CT), and ICG fluorescence imaging during and after surgery. Furthermore, in dogs where ICG fluorescence imaging was performed on the resected tracheobronchial lymph node, the size of the same node was evaluated from the preoperative CT images. Resected tissues obtained from all cases were used for the histopathological diagnosis. The occurrence of adverse events related to ICG administration during the intra- and postoperative periods was evaluated. No cases were excluded due to missing data in this study.

Informed consent was obtained from all the owners and information about all the procedures were provided to the owners. All the procedures were approved by the Ethical Committee of Nihon University Animal Medical Center.

2.2. ICG fluorescence imaging

Approximately 12–24 h before surgery, ICG (Diagnogreen; Daiichi Sankyo Co. Ltd., Tokyo, Japan) was diluted to 5 mg/mL



with distilled water for injection, and 2.0 mg/kg was administered intravenously. During surgery, pulmonary masses were observed visually in the lobes of the lungs exposed by thoracotomy. For the confirmed pulmonary masses, the lung surface was observed with an infrared camera system (HyperEye Medical System; Mizuho Medical Co. Ltd, Tokyo, Japan) before surgical resection (Figure 1). When images were taken, the surgical light was turned off and images were taken at a distance of 30–50 cm from the lung surface. Regardless of the fluorescent findings, pulmonary masses and lymph nodes, for which surgical resection was indicated, were removed. The resection margins of the pulmonary masses in the body were also imaged under the same conditions. The excised masses and lymph nodes were imaged under the same conditions in a shaded box, and the fluorescence was compared.

The fluorescence intensity was defined as 1 when it was stronger than the surrounding normal lung tissue, 0 when it was equivalent, and –1 when it lacked fluorescence. A score of 1 was defined as “fluorescent”, while 0 and –1 were defined as “no fluorescence”.

2.3. Histopathological diagnosis

Tissue samples were immersed in 10% neutral buffered formalin for 48 h and then embedded in paraffin. After the sections were deparaffinized with xylene, they were immersed in ethanol. The slides were stained with hematoxylin and eosin and subjected to histopathological testing. The histopathological findings were then compared with fluorescence findings.

2.4. Statistical analyses

The sensitivity, specificity and accuracy of complete resection using ICG fluorescence imaging were calculated for the cases in which fluorescence of the resected margin was evaluated. In addition, the chi-square test was used to analyze the relationship between ICG fluorescence of the resected margin and complete resection. Similarly, for cases in which lymph node fluorescence was evaluated, the sensitivity, specificity and accuracy of regional lymph node metastasis detection by ICG fluorescence imaging were calculated, and the

TABLE 1 Breeds of cases.

Breed	Number of cases
Miniature Dachshunds	9
Pembroke Welsh Corgis	6
Miniature Schnauzers	3
Border Collies	3
Mixed Breeds	3
Toy Poodles	2
French Bulldogs	2
Labrador Retrievers	2
American Cocker Spaniel	1
Golden Retriever	1
Bernese Mountain Dog	1
Pekingese	1
Shih Tzu	1
Flat Coated Retriever	1
Beagle	1
Jack Russell Terrier	1
Pomeranian	1
Chihuahua	1

chi-square test was performed to analyze the relationship between ICG fluorescence and histopathology of metastasis in the regional lymph nodes. The cutoff value of the size of the tracheobronchial lymph node in CT imaging was set to 12 mm based on a previous report (21). Accordingly, the sensitivity, specificity and accuracy of CT imaging for detection of tracheobronchial lymph node metastasis were calculated, and the chi-square test was used to analyze the relationship between CT findings and histopathology of metastasis in the tracheobronchial lymph nodes. SPSS Statistics 27 (IBM, Brussels, Belgium) was used for the analysis. Statistical significance was set at $p < 0.05$.

3. Results

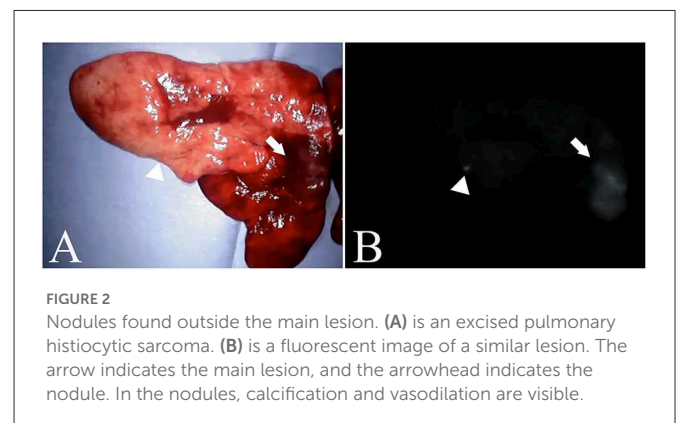
The median age of the dogs was 12.5 year-old [range: 6.4–15.7], and their median body weight was 7.8 kg [range: 1.9–36.3]. There were 19 spayed females, one intact female, 17 castrated males, and three intact males. The 40 dog breeds are summarized in Table 1. The median time from preoperative CT scan to surgery was 6 days [range: 0–41]. The median maximum diameter of the pulmonary masses on CT was 43.1 mm [range: 8.8–165.1].

Surgical procedures performed are summarized in Table 2. In one of the dogs that underwent resection of the right caudal lobe, a tumor was found in the left caudal lobe 1,110 days after surgery; therefore, resection of the left caudal lobe was performed.

A total of 44 nodules were resected from 40 dogs with pulmonary masses. Histopathologically, 32 nodules were diagnosed as lung adenocarcinoma, five were histiocytic sarcoma, three were undifferentiated sarcoma, two were malignant epithelial tumor metastases, and one was a carcinosarcoma. One nodule was a

TABLE 2 Surgical procedures for lung lobectomy.

Surgical procedures	Number of cases
Resection of the left cranial lobe	12
Resection of the left caudal lobe	10
Resection of the right caudal lobe	5
Resection of the right cranial lobe	3
En bloc resection of the right cranial and middle lobes	3
Left pneumonectomy	2
Resection of the right accessory lobe	2
Resection of the right middle lobe	1
Resection of the right middle lobe and en bloc resection of right caudal and accessory lobes	1
Resection of the left cranial lobe and right accessory lobe	1



non-tumoral lesion, and histopathology showed a collection of foamy macrophages.

The ICG fluorescence imaging was feasible in all dogs. In addition, all dogs showed no complications related with ICG fluorescence imaging. Each main lung mass in all dogs had a score of 1 for fluorescence intensity. Additional fluorescent nodules apart from the main lung mass were observed in four dogs (Figure 2). Of the four dogs, two dogs with lung adenocarcinoma as a main lesion had another fluorescent nodule: the nodule was metastasis of adenocarcinoma in one dog, but a non-tumoral lesion in another dog. One dog with histiocytic sarcoma as a main lesion had another fluorescent nodule which was a non-tumoral lesion, and the other dog had a large metastatic lung mass from mammary tumors as a main lesion and four other metastatic fluorescent nodules. In the four dogs with the fluorescent nodules apart from the main lesion, the contrast-enhanced CT revealed both nodules in two dogs with lung adenocarcinoma and three out of four nodules in the dog with metastases from the mammary tumors. In contrast, the residual one nodule in the dog with metastasis from the mammary tumors and one nodule in the dog with histiocytic sarcoma were not detected by the contrast-enhanced CT. The non-tumoral fluorescent nodules apart from the main lesion included calcification, ossification, and dilation of the blood vessels revealed by the histopathological examination.

In 23 nodules, fluorescence of the resection margin was compared with the evaluation of the surgical margin, and two of the three

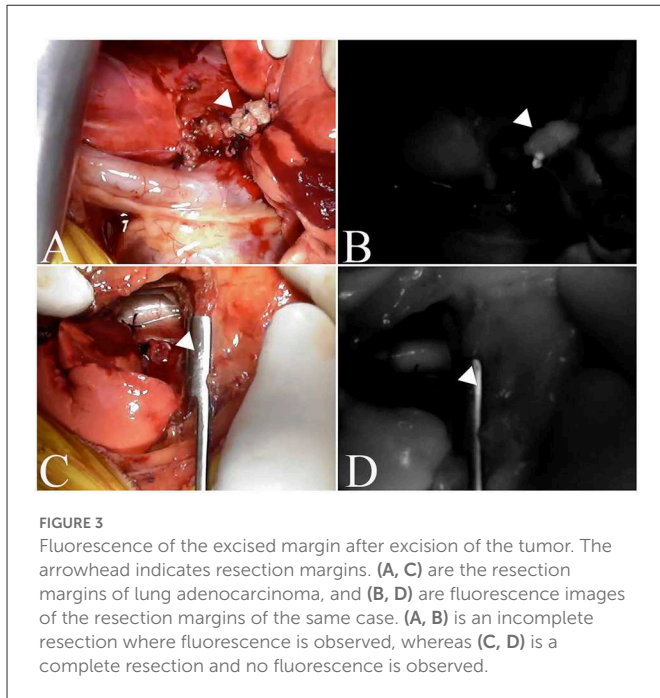


FIGURE 3

Fluorescence of the excised margin after excision of the tumor. The arrowhead indicates resection margins. (A, C) are the resection margins of lung adenocarcinoma, and (B, D) are fluorescence images of the resection margins of the same case. (A, B) is an incomplete resection where fluorescence is observed, whereas (C, D) is a complete resection and no fluorescence is observed.

nodules with incomplete resection showed fluorescence, while one nodule did not (Figure 3). Of the 20 nodules with complete resection, eight nodules showed fluorescence, while 12 nodules did not. The sensitivity, specificity and accuracy of ICG fluorescence for complete resection of pulmonary tumors were found to be 66.7, 60.0, and 60.9%, respectively. There was not a significant relationship between ICG fluorescence of the resected margin and complete resection ($p = 0.3849$).

Lymphadenectomy was performed in 11 dogs, and 13 lymph nodes were removed. Of these, 11 were tracheobronchial lymph nodes and two were cranial mediastinal lymph nodes. Histopathologically, metastatic lesions were found in five of the tracheobronchial lymph nodes.

Seven lymph nodes (six tracheobronchial lymph nodes and one cranial mediastinal lymph node) resected from six dogs whose lymph node fluorescence was evaluated were compared in terms of the presence of metastasis. Fluorescence was observed in all three nodes with metastasis, whereas fluorescence was observed in only one of four nodes without metastasis; no fluorescence was observed in the remaining three nodes (Figure 4). The sensitivity, specificity and accuracy of ICG fluorescence for evaluating lymph node metastasis of pulmonary tumors were found to be 100, 75.0, and 85.7%, respectively. There was a significant relationship between ICG fluorescence and histopathological metastasis of the lymph nodes ($p = 0.0472$).

The size on CT images and fluorescence of tracheobronchial lymph nodes are summarized in Table 3. The median size of the six tracheobronchial lymph nodes evaluated for fluorescence on CT images was 8.0 mm [range: 4.6–18.3]. For these cases, the median maximum diameter of the pulmonary masses on CT images was 35.4 mm [range: 30.1–42.0]. When the cutoff value of the tracheobronchial lymph node size was set at 12 mm, the sensitivity, specificity and accuracy of the diameter of the pulmonary mass on CT for detection of lymph node metastasis was 33.3, 100, and 66.7%, respectively. There was not a significant relationship

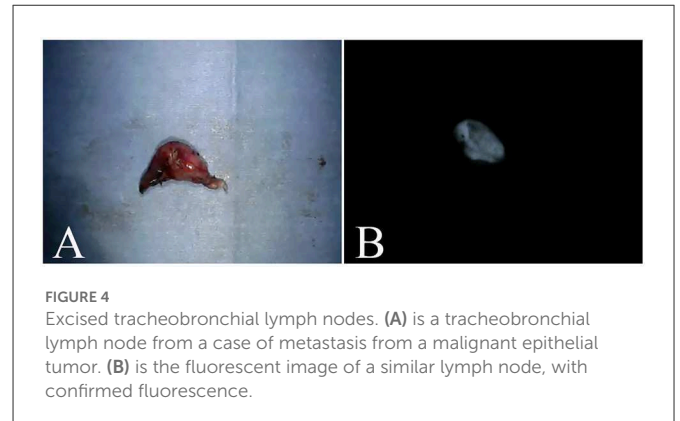


FIGURE 4

Excised tracheobronchial lymph nodes. (A) is a tracheobronchial lymph node from a case of metastasis from a malignant epithelial tumor. (B) is the fluorescent image of a similar lymph node, with confirmed fluorescence.

between CT findings and histopathological metastasis of the lymph nodes ($p = 0.2733$).

4. Discussion

All pulmonary tumors showed the ICG fluorescence irrespective of histopathological diagnosis; therefore, it was possible to intraoperatively identify the degree of infiltration of pulmonary tumors. However, most masses were lung adenocarcinoma, with only a few other lesion types in our study. Therefore, further clinical studies are required to clarify the usefulness of ICG fluorescence in differential diagnosis of lung tumors.

The mechanism by which ICG fluoresces in tumors remains unclear in the field of human medicine. It is believed that anion-transporting peptides, intracellular transporters, and export transporters are involved in the mechanism by which hepatic tumors exhibit ICG fluorescence in human medicine (22). In contrast, the enhanced permeability and retention (EPR) effect has been suggested as the mechanism by which tumors other than hepatic tumors exhibit ICG fluorescence (23). The EPR effect is a property by which small molecules such as ICG, which are injected systemically and passively, accumulate in tumors due to the presence of defective endothelial cells and wide fenestrations (600–800 nm) in nascent blood vessels (24). In our study, the accumulation of ICG particles in tumors due to the EPR effect was thought to be responsible for fluorescence in all tumors. Fluorescence was also observed in non-tumor, macrophage-associated nodules; however, tumor and inflammatory tissues have been reported to undergo similar vascular changes in the microenvironment (25). A phenomenon similar to the EPR effect may have occurred in this nodule showing fluorescence. Nevertheless, it is necessary to investigate the fluorescence mechanism of ICG in pulmonary tumors in dogs.

Our study demonstrated a low diagnostic accuracy for the complete resection of lung tumors in dogs. Since there were only a few cases in which the fluorescence of the excised margin was evaluated, it is necessary to further increase the sample size in future studies. Furthermore, the percentage of false positives (cases in which fluorescence was observed at the resection margin despite being a complete resection) was high. In humans, a previous study reported that ICG is metabolized in the liver, resulting in shorter visualization times in the lungs (26). Moreover, it has been reported that ICG can be administered intravenously at 1–5 mg/kg for the fluorescence imaging of human pulmonary tumors (27–29). The

TABLE 3 Size on CT images and fluorescence of tracheobronchial lymph nodes.

Lymph node no.	Histopathological diagnosis of main lesion	Metastasis	Size on CT images (mm)	Fluorescence
#1	Lung adenocarcinoma	No	6.9	No
#2	Lung adenocarcinoma	No	7.8	No
#3	Lung adenocarcinoma	Yes	4.6	Yes
#4	Lung adenocarcinoma	No	8.2	Yes
#5	Histiocytic sarcoma	Yes	11.3	Yes
#6	Metastases of malignant epithelial tumor	Yes	18.3	Yes

CT, computed tomography.

maximum dose of ICG for intravenous injection in humans is set at 5.0 mg/kg (30–34). In addition, the occurrence rate of allergic reactions with doses below 0.5 mg/kg was reported as 0.003%, which increased significantly when the dose exceeded 5.0 mg/kg (35). In a previous study, 5.0 mg/kg of ICG was administered for the fluorescence imaging of canine pulmonary tumors (36). No adverse event was observed at the ICG dose of 2.0 mg/kg used in our study. However, further investigations are required to establish the optimal dose of ICG for fluorescence imaging in canine pulmonary tumors. Determining the optimal ICG dose may improve its sensitivity and specificity in the evaluation of the complete resection.

Our study revealed that the presence of lymph node metastasis could be determined with a high probability by assessing ICG fluorescence observation of the lymph nodes. When lymph node fluorescence was observed, there was a tendency for the size of the lymph node on CT to increase. A previous study reported that metastasis to tracheobronchial lymph nodes can be evaluated by CT imaging with a sensitivity of 85.7% and specificity of 95.2% in dogs (21); however, when measured under the same conditions in the present study, the sensitivity was low. In lymph node metastasis of lung tumors in dogs, the ICG fluorescence method was sensitive, whereas a previous study reported that CT had high specificity (21). Therefore, better results might be obtained by combining these two methods. However, our study did not conclude that the combination of ICG fluorescence and CT imaging may be useful because of the low sensitivity of CT for lymph node metastasis. There was no significant relationship between the size of tracheobronchial lymph nodes in the CT imaging and the presence of lymph node metastasis, while there was a significant relationship between ICG fluorescence of the lymph nodes and the presence of lymph node metastasis. In human medicine, ICG fluorescence has also been used for sentinel lymph node mapping in pulmonary tumors (37). The identification rate of sentinel lymph nodes for human pulmonary tumor using isosulfanblue is low (22–50%) (37). In contrast, ICG administered intraoperatively around the tumor has been reported to have an identification rate of 80.7% (38). In our study, ICG was administered intravenously before surgery. Intravenously administered ICG is thought to be moved into the tumor cells by the EPR effect and then flow into the lymphatic vessels, which may produce the ICG fluorescence in the regional lymph nodes. Our study suggests that, like intraoperative peri-tumoral injection of ICG, intravenous administration of ICG can be used for sentinel lymph node mapping of canine lung tumors. However, our study did not investigate the difference in fluorescence between intraoperative peri-tumoral and preoperative intravenous administration of ICG. Therefore, further studies are warranted to clarify the optimal route of ICG

administration for the intraoperative identification of lung tumor and sentinel lymph node mapping in dogs.

The limitations of our study include the small number of cases in which the intraoperative and postoperative conditions of the dogs allowed evaluation of the fluorescence of the resected margins and lymph nodes. The suitable dose and duration of ICG administration are still controversial.

In conclusion, ICG fluorescence imaging might be a useful intraoperative diagnostic method to identify tumor location and lymph node metastasis, but not for evaluation of the complete resection in dogs with pulmonary malignant tumors.

Data availability statement

The original contributions presented in the study are included in the article/supplementary material, further inquiries can be directed to the corresponding author.

Ethics statement

The animal study was reviewed and approved by Ethical Committee of Nihon University Animal Medical Center. Written informed consent was obtained from the owners for the participation of their animals in this study.

Author contributions

KA and KI contributed to designing and planning the study, participated in the surgeries and peri-operative management, wrote, and reviewed the manuscript. NS contributed to designing and planning the study, participated in the surgeries and peri-operative management, and wrote the manuscript. KT, TH, and OY contributed to supporting the study and participated in the surgeries and peri-operative management. YK and KO contributed to evaluating histopathological examination. All authors contributed to the article and approved the submitted version.

Conflict of interest

YK and KO are employed by the company North Lab.

The remaining authors declare that this research was carried out in the absence of any commercial or financial relationships that could be construed as a potential conflict of interest.

Publisher's note

All claims expressed in this article are solely those of the authors and do not necessarily represent those of their affiliated

organizations, or those of the publisher, the editors and the reviewers. Any product that may be evaluated in this article, or claim that may be made by its manufacturer, is not guaranteed or endorsed by the publisher.

References

- Landsman ML, Kwant G, Mook GA, Zijlstra WG. Light-absorbing properties, stability, and spectral stabilization of indocyanine green. *J Appl Physiol.* (1976) 40:575–83. doi: 10.1152/jappl.1976.40.4.575
- Ishizawa T, Fukushima N, Shibahara J, Masuda K, Tamura S, Aoki T, et al. Real-time identification of liver cancers by using indocyanine green fluorescent imaging. *Cancer.* (2009) 115:2491–504. doi: 10.1002/cncr.24291
- Ishizawa T, Saiura A, Kokudo N. Clinical application of indocyanine green-fluorescence imaging during hepatectomy. *Hepatobiliary Surg Nutr.* (2016) 5:322–8. doi: 10.21037/hbsn.2015.10.01
- Paruch K, Dang JT, Poonja A, Sun WYL, Bigam D, Birch D, et al. Intraoperative fluorescence imaging with indocyanine green in hepatic resection for malignancy: a systematic review and meta-analysis of diagnostic test accuracy studies. *Surg Endosc.* (2020) 34:2891–903. doi: 10.1007/s00464-020-07543-2
- Ito N, Fukuta M, Tokushima T, Nakai K, Ohgi S. Sentinel node navigation surgery using indocyanine green in patients with lung cancer. *Surg Today.* (2004) 34:581–5. doi: 10.1007/s00595-004-2780-y
- Kitai T, Inomoto T, Miwa M, Shikayama T. Fluorescence navigation with indocyanine green for detecting sentinel lymph nodes in breast cancer. *Breast Cancer.* (2005) 12:211–5. doi: 10.2325/jbcs.12.211
- Nimura H, Narimiya N, Mitsumori N, Yamazaki Y, Yanaga K, Urashima M. Infrared ray electronic endoscopy combined with indocyanine green injection for detection of sentinel nodes of patients with gastric cancer. *Br J Surg.* (2004) 91:575–9. doi: 10.1002/bjs.4470
- Parungo CP, Ohnishi S, Kim SW, Kim S, Laurence RG, Soltész EG, et al. Intraoperative identification of esophageal sentinel lymph nodes with near-infrared fluorescence imaging. *J Thorac Cardiovasc Surg.* (2005) 129:844–50. doi: 10.1016/j.jtcvs.2004.08.001
- Rubens FD, Ruel M, Frenes SE. A new and simplified method for coronary and graft imaging during CABG. *Heart Surg Forum.* (2002) 5:141–4.
- Iida G, Asano K, Seki M, Ishigaki K, Teshima K, Yoshida O, et al. Intraoperative identification of canine hepatocellular carcinoma with indocyanine green fluorescent imaging. *J Small Anim Pract.* (2013) 54:594–600. doi: 10.1111/jsap.12148
- Steffey MA, Mayhew PD. Use of direct near-infrared fluorescent lymphography for thoracoscopic thoracic duct identification in 15 dogs with chylothorax. *Vet Surg.* (2018) 47:267–76. doi: 10.1111/vsu.12740
- Townsend KL, Milovancev M, Bracha S. Feasibility of near-infrared fluorescence imaging for sentinel lymph node evaluation of the oral cavity in healthy dogs. *Am J Vet Res.* (2018) 79:995–1000. doi: 10.2460/ajvr.79.9.995
- Suh YJ, Choi JY, Chai YJ, Kwon H, Woo JW, Kim SJ, et al. Indocyanine green as a near-infrared fluorescent agent for identifying parathyroid glands during thyroid surgery in dogs. *Surg Endosc.* (2015) 29:2811–7. doi: 10.1007/s00464-014-3971-2
- Quinlan ASF, Wainberg SH, Phillips E, Oblak ML. The use of near infrared fluorescence imaging with indocyanine green for vascular visualization in caudal auricular flaps in two cats. *Vet Surg.* (2021) 50:677–86. doi: 10.1111/vsu.13577
- Wakaiki S, Maehara S, Abe R, Tsuzuki K, Igarashi O, Saito A, et al. Indocyanine green angiography for examining the normal ocular fundus in dogs. *J Vet Med Sci.* (2007) 69:465–70. doi: 10.1292/jvms.69.465
- Vail DM, Thamm D, Liptak JM. Pulmonary neoplasia. In: *Withrow and MacEwen's Small Animal Clinical Oncology*. 6th ed. Philadelphia: Saunders (2019) p. 507–23.
- Barrett LE, Pollard RE, Zwingenberger A, Zierenberg-Ripoll A, Skorupski KA. Radiographic characterization of primary lung tumors in 74 dogs. *Vet Radiol Ultrasound.* (2014) 55:480–7. doi: 10.1111/vru.12154
- McNiel EA, Ogilvie GK, Powers BE, Hutchison JM, Salman MD, Withrow SJ. Evaluation of prognostic factors for dogs with primary lung tumors: 67 cases (1985–1992). *J Am Vet Med Assoc.* (1997) 211:1422–7.
- Johnston SA, Tobias KM. Pulmonary neoplasia. In: *Veterinary Surgery: Small Animal*. 2nd ed. Philadelphia: Saunders (2017) p. 4637–44.
- Polton GA, Brearley MJ, Powell SM, Burton CA. Impact of primary tumour stage on survival in dogs with solitary lung tumours. *J Small Anim Pract.* (2008) 49:66–71. doi: 10.1111/j.1748-5827.2007.00403.x
- Ballegeer EA, Adams WM, Dubielzig RR, Paoloni MC, Klauer JM, Keuler NS. Computed tomography characteristics of canine tracheobronchial lymph node metastasis. *Vet Radiol Ultrasound.* (2010) 51:397–403. doi: 10.1111/j.1740-8261.2010.01675.x
- Ishizawa T, Masuda K, Urano Y, Kawaguchi Y, Satou S, Kaneko J, et al. Mechanistic background and clinical applications of indocyanine green fluorescence imaging of hepatocellular carcinoma. *Ann Surg Oncol.* (2014) 21:440–8. doi: 10.1245/s10434-013-3360-4
- Jiang JX, Keating JJ, Jesus EMD, Judy RP, Madajewski B, Venegas O, et al. Optimization of the enhanced permeability and retention effect for near-infrared imaging of solid tumors with indocyanine green. *Am J Nucl Med Mol Imaging.* (2015) 5:390–400.
- Matsumura Y, Maeda H. A new concept for macromolecular therapeutics in cancer chemotherapy: mechanism of tumorotropic accumulation of proteins and the antitumor agent smancs. *Cancer Res.* (1986) 46:6387–92.
- Hanahan D, Weinberg RA. The hallmarks of cancer. *Cell.* (2000) 100:57–70. doi: 10.1016/S0092-8674(00)81683-9
- Cui F, Liu J, Du M, Fan J, Fu J, Geng Q, et al. Expert consensus on indocyanine green fluorescence imaging for thoracoscopic lung resection (The Version 2022). *Transl Lung Cancer Res.* (2022) 11:2318–31. doi: 10.21037/tlcr-22-810
- Kim HK, Quan YH, Choi BH, Park JH, Han KN, Choi Y, et al. Intraoperative pulmonary neoplasm identification using near-infrared fluorescence imaging. *Eur J Cardiothorac Surg.* (2016) 49:1497–502. doi: 10.1093/ejcts/evz367
- Okusanya OT, DeJesus EM, Jiang JX, Judy RP, Venegas OG, Deshpande CG, et al. Intraoperative molecular imaging can identify lung adenocarcinomas during pulmonary resection. *J Thorac Cardiovasc Surg.* (2015) 150:28–35.e1. doi: 10.1016/j.jtcvs.2015.05.014
- Predina JD, Keating J, Patel N, Nims S, Singhal S. Clinical implications of positive margins following non-small cell lung cancer surgery. *J Surg Oncol.* (2016) 113:264–9. doi: 10.1002/jso.24130
- Keating JJ, Runge JJ, Singhal S, Nims S, Venegas O, Durham AC, et al. Intraoperative near-infrared fluorescence imaging targeting folate receptors identifies lung cancer in a large-animal model. *Cancer.* (2017) 123:1051–60. doi: 10.1002/cncr.30419
- Lim C, Vibert E, Azoulay D, Salloum C, Ishizawa T, Yoshioka R, et al. Indocyanine green fluorescence imaging in the surgical management of liver cancers: current facts and future implications. *J Visc Surg.* (2014) 151:117–24. doi: 10.1016/j.jvisurg.2013.11.003
- Newton AD, Predina JD, Frenzel-Sulyok LG, Shin MH, Wang Y, Singhal S. Intraoperative near-infrared imaging can identify sub-centimeter colorectal cancer lung metastases during pulmonary metastasectomy. *J Thorac Dis.* (2018) 10:E544–8. doi: 10.21037/jtd.2018.06.161
- Okusanya OT, Holt D, Heitjan D, Deshpande C, Venegas O, Jiang J, et al. Intraoperative near-infrared imaging can identify pulmonary nodules. *Ann Thorac Surg.* (2014) 98:1223–30. doi: 10.1016/j.athoracsur.2014.05.026
- Predina JD, Newton AD, Corbett C, Xia L, Shin M, Sulfyok LE, et al. A clinical trial of TumorGlow to identify residual disease during pleurectomy and decortication. *Ann Thorac Surg.* (2019) 107:224–32. doi: 10.1016/j.athoracsur.2018.06.015
- Pischik VG, Kovalenko A. The role of indocyanine green fluorescence for intersegmental plane identification during video-assisted thoracoscopic surgery segmentectomies. *J Thorac Dis.* (2018) 10:S3704–11. doi: 10.21037/jtd.2018.04.84
- Holt D, Okusanya O, Judy R, Venegas O, Jiang J, DeJesus E, et al. Intraoperative near-infrared imaging can distinguish cancer from normal tissue but not inflammation. *PLoS ONE.* (2014) 9:e103342. doi: 10.1371/journal.pone.0103342
- Gregor A, Ujiié H, Yasufuku K. Sentinel lymph node biopsy for lung cancer. *Gen Thorac Cardiovasc Surg.* (2020) 68:1061–78. doi: 10.1007/s11748-020-01432-0
- Yamashita S, Tokuiishi K, Anami K, Miyawaki M, Moroga T, Kamei M, et al. Video-assisted thoracoscopic indocyanine green fluorescence imaging system shows sentinel lymph nodes in non-small-cell lung cancer. *J Thorac Cardiovasc Surg.* (2011) 141:141–4. doi: 10.1016/j.jtcvs.2010.01.028